Materials Science and Engineering B 184 (2014) 1–6

Contents lists available at ScienceDirect

Materials Science and Engineering B

journal homepage: www.elsevier.com/locate/mseb

A facile one-step method for synthesising a parallelogram-shaped single-crystalline ZnO nanosheet

Renyun Zhang*, Magnus Hummelgård, Håkan Olin

Department of Natural Sciences, Mid Sweden University, SE-85170 Sundsvall, Sweden

ARTICLE INFO

Article history:
Received 4 October 2013
Received in revised form
10 December 2013
Accepted 15 December 2013
Available online 28 January 2014

Keywords:
Zinc oxide
Nanostructured materials
Atomic force microscopy
Transmission electron microscopy

ABSTRACT

ZnO nanosheets are found to be useful in many fields such as sensors and electronics. Non-uniform-shaped ZnO nanosheets are synthesised using several methods; moreover, uniformly shaped ones are less studied. Here, we report on a simple one-step method to synthesise parallelogram-shaped single-crystalline ZnO nanosheets. By controlling the reaction of $Zn(NO_3)_2$ and hexamethylenetetramine (HMT) in ethanol, average 30 nm-thick nanosheets with a high aspect ratio of 1:100 were obtained. The parallelogram angles were between 97° and 99°. Transmission electron microscopy (TEM) diffraction and X-ray diffraction (XRD) showed that the nanosheets were wurtzite-structured single-crystalline ZnO. Moreover, a growth mechanism of these parallelogram nanosheets is suggested based on the experimental results. These results suggest a new simple solution process to synthesise uniformly shaped ZnO nanosheets allowing large-scale production to be employed.

1. Introduction

The zinc oxide (ZnO) nanomaterial is an interesting metal oxide, with several scientific and engineering-based applications. To synthesise ZnO nanostructures, several methods have been developed to obtain the desired zero-, one- and two-dimensional nanostructures. Zero-dimensional ZnO nanoparticles are mainly synthesised by wet chemical methods [1,2], while one-dimensional ZnO nanowires/nanorods can be synthesised by physical vapour deposition (PVD) [3], thermal evaporation [4], wet chemical methods [5,6] or modified wet chemical methods [7,8]. Two-dimensional ZnO nanosheets/nanodiscs/nanoplates could also be made by PVD [9] or wet chemical methods [10,11].

Two-dimensional ZnO nanosheets are ideal nanomaterials for the fabrication of nanodevices [9,12–15], with applications in electronics [16,17], optics [18] and photonics [19]. High-quality thin ZnO nanosheets have large parallel planar defect-free surfaces and are also attractive materials due to their high mechanical and thermal stability [20]. There are several methods to synthesise large-sized single-crystalline ZnO nanosheets [19], such as vapour-transportation deposition [20], PVD [9], hydrothermal method [10,21,22] and non-water-based wet chemical method [23]. The synthesised nanosheets could be irregular [10] or of regular shape such as rectangular [20] or hexagonal sheets [24,25]. To obtain regular-shaped ZnO nanosheets using high-temperature physical methods, there is a need for a specific substrate [24] or for several processing steps [20], which either limit the production quantity or increase the complexity. There are also wet methods to obtain dispersed ZnO hexagonal nanodiscs in which the growth of ZnO is suppressed in certain directions [26]; however, seeding nanoparticles are necessary to induce the growth of the nanodiscs. Some simpler methods have been developed to obtain hexagonal ZnO nanodiscs, but these nanodiscs have a low aspect ratio [27] or form stacked rods [28].

Although many kinds of ZnO nanodiscs or nanosheets are synthesised, there is a need for large-area, thin, regular-shaped, single-crystalline ZnO nanosheets for use in, for example, electronics [29]. Two-dimensional structures are also of importance in flexible electronics as they are less sensitive to bending [30] and are easily deposited on large-area substrates [31]. Large-area, thin, single-crystalline ZnO nanosheets have been obtained using the PVD method [23], but the production quantity is limited by the method. Wet chemical or solvent-based methods are promising for the production of larger quantities, but the produced nanosheets rarely have large area and thin thickness [27,28].

We report here on a solvent-based method capable of producing large amounts of large-sized, regular-shaped, single-crystalline ZnO nanosheets. The reaction between $Zn(NO_3)_2{\cdot}6H_2O$ and hexamethylenetetramine (HMT) was carried out in an ethanol solvent, while controlling the reaction temperature and during stirring. Thin parallelogram-shaped ZnO nanosheets with an aspect ratio of 1:100 were obtained at 60 °C in a solvent of 95% ethanol. These results demonstrate a simple method for synthesising uniformly shaped ZnO nanosheets.

* Corresponding author. Tel.: +46 60 148484; fax: +46 60 148802.
E-mail addresses: renyun.zhang@miun.se, zhang7901@gmail.com (R. Zhang).

0921-5107/$ – see front matter © 2013 Elsevier B.V. All rights reserved.
http://dx.doi.org/10.1016/j.mseb.2013.12.009

2. Experimental

2.1. Synthesis of ZnO nanosheets

ZnO nanosheets were synthesised in ethanol using HMT and $Zn(NO_3)_2{\cdot}6H_2O$ as reactants. Briefly, 0.2 g HMT and 0.2 g $Zn(NO_3)_2{\cdot}6H_2O$ were added in 200 ml 95% ethanol (commercial 95% ethanol, or mixture of 191 ml 99.5% ethanol and 9 ml double-distilled water). The beaker that contains the solid reactants was placed in an oven while stirring at 500 rpm. For control experiments, only double-distilled water or 99.5% ethanol was used as a solvent. The temperature was then increased from room temperature to 60 °C and kept at 60 °C for 1 h. Samples for characterisation were taken at 0 min (when the temperature just reached 60 °C), and then after 5, 10, 20, 40 and 60 min. The samples that were taken from the solution were centrifuged for 2 min at 6000 rpm, rinsed with double-distilled water three times and re-dispersed in ethanol. The detailed reaction between $Zn(NO_3)_2$ and HMT is [32]

$$(CH_2)_6N_4 + 6H_2O \rightarrow 6COH_2 + NH_3$$

$$NH_3 + H_2O \rightarrow NH_4^+ + OH^-$$

$$Zn(NO_3)_2 \rightarrow Zn^{2+} + 2NO_3^-$$

$$Zn^{2+} + 2OH^- \rightarrow ZnO + H_2O$$

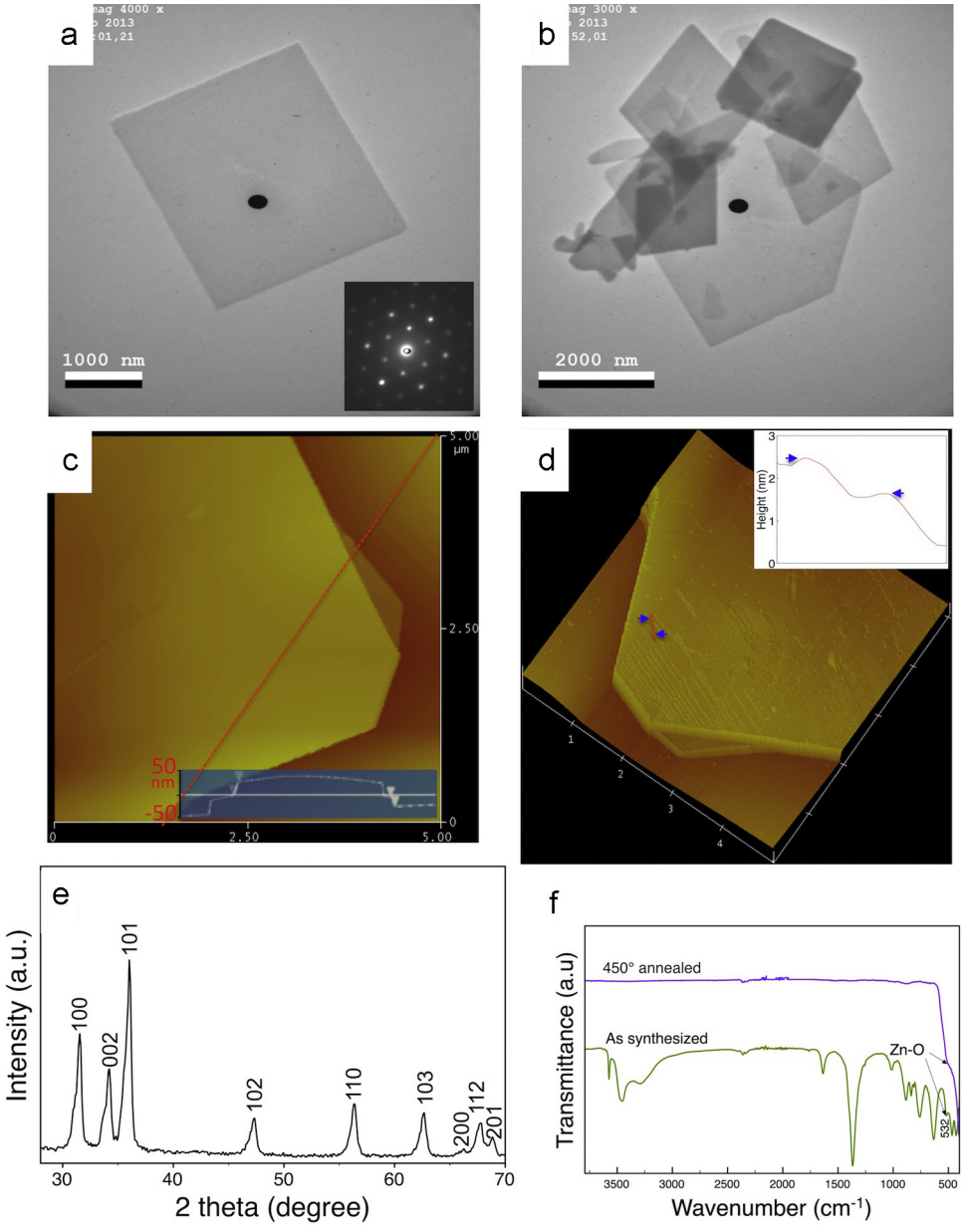

Fig. 1. Characterizations of ZnO nanosheets. (a) A TEM image of a parallelogram shaped single crystalline ZnO nanosheets. The insert shows an electron diffraction pattern of the nanosheets, indicating single crystals. The black dot in the center is an imaging artifact. (b) TEM image of several ZnO nanosheets with different sizes and transparency of nanosheets. (c) AFM image of two stacked ZnO nanosheets. The insert is a cross section of the red line in the image showing nanosheet thicknesses of 28 and 31 nm. (d) 3D view of the image in (c), where steps on the (0 0 1) plane were imaged. The cross section analysis of the image, as shown in the inset (d), indicating an average height of 0.9 per step. (e) XRD of ZnO nanosheets. (f) FTIR of ZnO nanosheets before and after annealed at 450 °C. (For interpretation of the references to colour in this figure legend, the reader is referred to the web version of the article.)

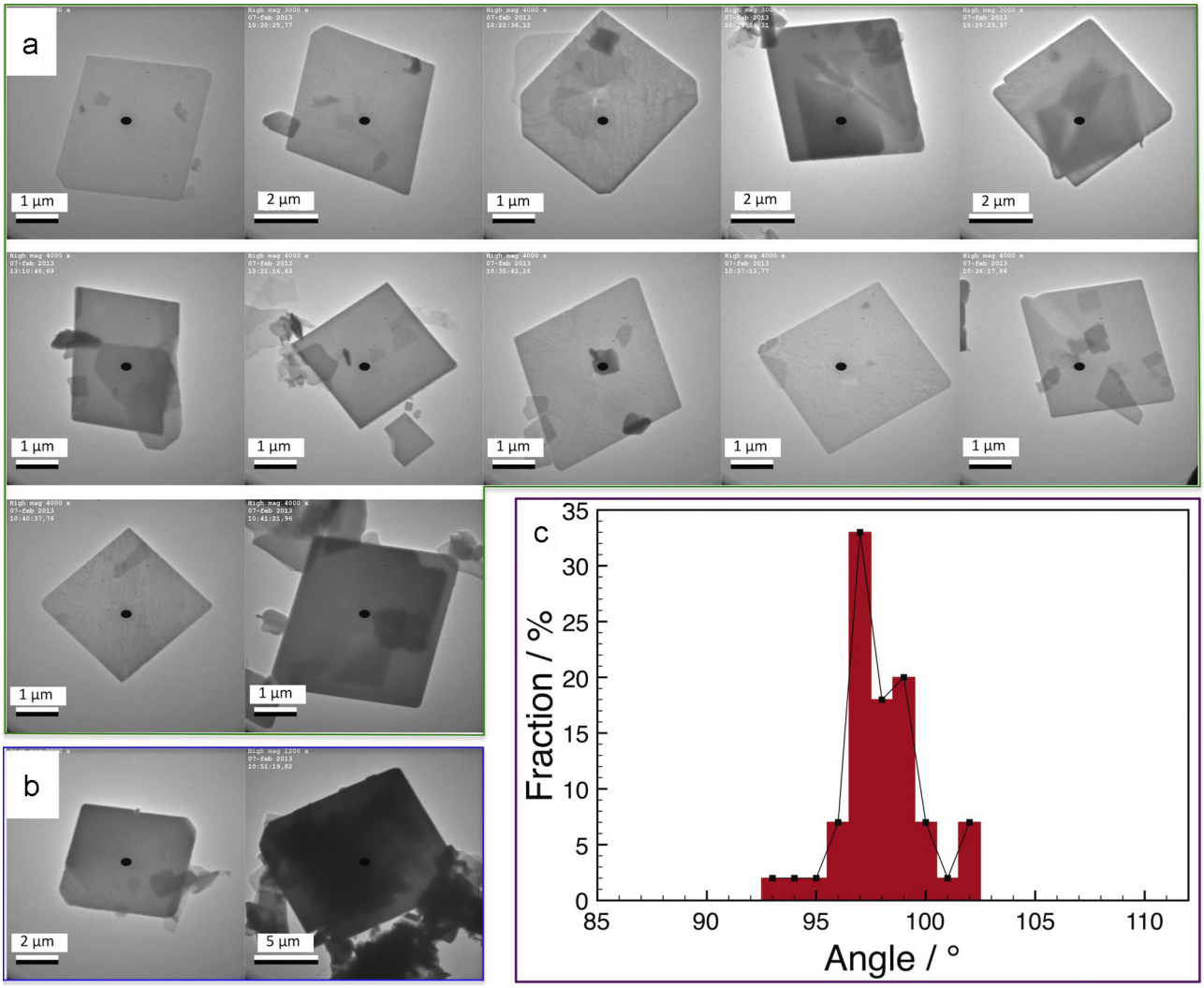

Fig. 2. (a) Some examples of synthesized ZnO nanosheets showing the most common shapes of the nanosheets. (b) Two ultra-large nanosheets, 6 μm × 5 μm and 13.3 μm × 11.3 μm. (c) Statistics of the obtuse angles of 40 nanosheets.

2.2. Characterisation

Transmission electron microscope (TEM) imaging was performed on a 2000FX (JEOL) microscope with an acceleration voltage of 160 kV. Atomic force microscope (AFM) imaging was done using a Nanoscope IIIa microscope (Veeco Instruments, Santa Barbara, CA, USA). Fourier transform infrared (FTIR) spectroscopy was done using a Nicolet 6700 (THERMAL) spectrometer. X-ray diffraction (XRD) was performed on a D2 Phaser (BRUKER) X-ray powder diffractometer.

3. Results and discussion

Using ethanol as a solvent [27], large-sized parallelogram-shaped single-crystalline ZnO nanosheets were synthesised within 1 h at 60 °C [28]. Fig. 1a shows a TEM image of a typically sized (2.7 μm × 2.8 μm) ZnO nanosheet, indicating a perfect parallelogram shape and a single-crystalline structure (inserted electron diffraction image in Fig. 1a). The typical thickness of these synthesised nanosheets was about 30 nm, but the range varied from 20 to 200 nm, as shown in Fig. 1b where the darkness is varying for different nanosheets. The aspect ratio between the length of the parallelogram sheet and the thickness was found to be about 1:100. The typical thickness of the synthesised nanosheet is about 30 nm after 1 h of the reaction (Fig. 1c); however, the thickness could increase at extended growth time. This increase of thickness was imaged with AFM, where the growth of the (0 0 1) planes was observed. The height of single (0 0 1) steps was about 0.9 nm (Fig. 1d), which is higher than the theoretical value of 0.52 nm [33]. Besides the thickness, we also found that the lateral sizes (the area of the sheets) varied in a large range, which will be discussed below.

XRD measurements (Fig. 1e) showed a wurtzite structure [29] of these ZnO nanosheets. The stronger peaks at 31.5°, 34.2° and 36° correspond to the (1 0 0), (0 0 2) and (1 0 1) planes of wurtzite ZnO, respectively [13]. The lattice spacing of the (0 0 2) planes was determined to be 2.61 Å and the lattice constants as $a = 3.275$ Å and $c = 5.24$ Å, with $c/a = 1.601$, indicating a wurtzite structure [34]. FTIR results (Fig. 1f) indicated a Zn—O stretching [35] at a wave number of 532 cm^{-1} which was measured after 450 °C annealing. The annealing removed the groups from HMT and the –OH groups on ZnO nanosheets.

Fig. 2a lists some examples of typical parallelogram ZnO nanosheets (a low-magnification TEM image is given in supporting information as Fig. S1), where we can find that besides perfectly shaped parallelogram there are less ideally shaped nanosheets. This could be due to the suppressed crystalline growth at certain directions. Fig. 2b shows two large nanosheets with areas of 22 and 147 μm^2. With such large areas, one can easily build

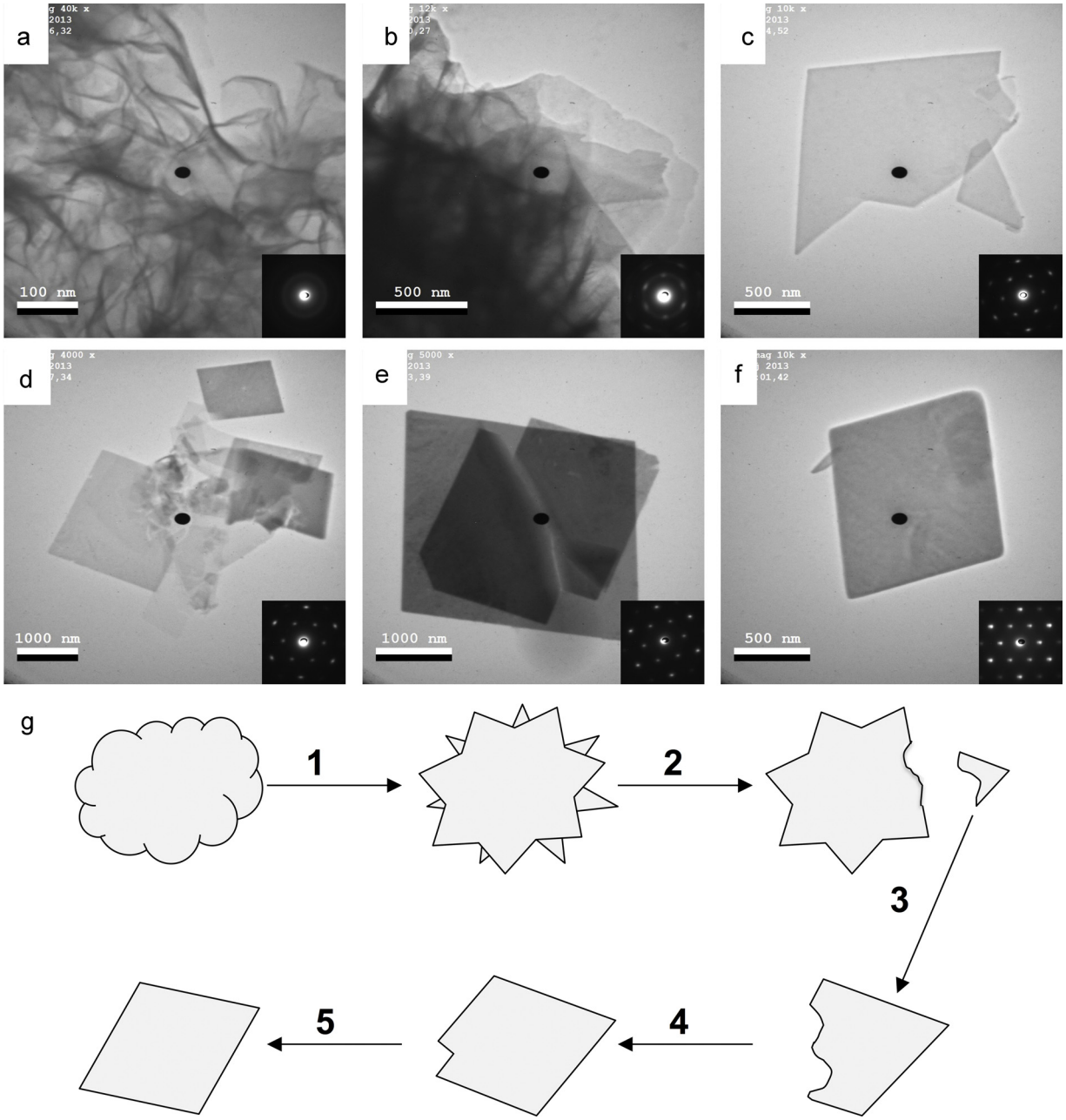

Fig. 3. The growth process of the ZnO nanosheets. (a)–(f) TEM images of the samples at reaction time of (a) 0 minute after the temperature just reached 60 °C, (b) 5 min, (c) 10 min, (d) 20 min, (e) 40 min, and (f) 60 min. The insets show the electron diffraction patterns of the samples. (g) A schematic drawing of the possible process steps. Thin soft sheets was first obtained when the temperature reached 60 °C, and then the sheets became harder at step 1 after some time. At step 2, the shear force generated by the stirring broke the hard thin film, resulting in smaller flakes. At step 3, and 4, the smaller flakes grew toward the parallelogram shape completed at step 5.

electronics with the aid of some instruments. Although the size of the nanosheet varies in a wide range, the angles of the parallelograms were limited in a narrow range. Fig. 2c shows the statistic results of 40 different-sized parallelogram nanosheets, the angles of which were mostly between 97° and 99° although the whole range was found to be between 93° and 103°.

Usually, growth of ZnO crystals in solvents prefers the (0 0 1) direction, because of the low surface energy [36]. To obtain nanosheets or nanodiscs in solution, some reagents, such as sodium citrate, are needed to suppress the growth of ZnO in the (0 0 1) facet [27]. However, in our study, no extra reagent was added. We used 95% ethanol (95% ethanol or diluted from 99.5% ethanol) as a solvent and let the reaction to occur at 60 °C while stirring (500 rpm). The dissolving speeds of both $Zn(NO_3)_2{\cdot}6H_2O$ and HMT in ethanol are slower than in water, which slowed down the reaction speed, avoiding high-speed growth of ZnO in the (0 0 1) direction. At the beginning, when the reaction solution was placed in an oven and the temperature increased from room temperature to 60 °C, the two reactants dissolved and formed the thin-layered structures as imaged with TEM (Fig. 3a). These thin-layered structures were very soft and without crystalline structures. When the reaction continued, the thin layers started to form sheet-like structures (Fig. 3b) 5 min after the temperature reached 60 °C. A polycrystalline structure was observed, as shown in the diffraction pattern inserted in Fig. 3b. Single-crystalline ZnO nanosheets were found 10 min after the temperature reached 60 °C; however, the nanosheets did not have a perfect parallelogram structure (Fig. 3c). After another 10 min, we found that the nanosheets were

growing towards a perfect parallelogram shape (Fig. 3d) and observed some perfectly parallelogram-shaped nanosheets. A large amount of parallelogram-shaped nanosheets appeared 40 min after the temperature reached 60 °C (Fig. 3e). The reaction was stopped after 1 h at 60 °C, and the bulk amount of parallelogram-shaped nanosheets (Fig. 3f) was collected by filtration.

Fig. 3g shows the possible growing processes of the parallelogram-shaped ZnO nanosheets. At the beginning, the two reactants dissolve in ethanol and form soft layers, which might be due to the structure change of the HMT when it reacts with $Zn(NO_3)_2$. The reaction between HMT and $Zn(NO_3)_2$ takes several steps, because there are several sites on HMT that can react with $Zn(NO_3)_2$. When most of the sites are reacted with $Zn(NO_3)_2$, the soft thin layer becomes harder thin sheets. The shear force generated by stirring breaks the hard thin sheets, leading to many incomplete ZnO sheets, as shown in Fig. 3c. Moreover, because of the large range of sizes of the broken sheets, the final parallelogram-shaped nanosheets were also differently sized. When these incomplete sheets are in to the reaction solution, the growth of ZnO nanosheets is towards a perfect parallelogram shape.

One important phenomenon that should be pointed out is that the thicknesses of the nanosheets are increasing all the time. As shown in Fig. 3, we found that the transparency of the nanosheets was decreasing, which means the thickness was increasing. This observation is in agreement with our AFM results, where we imaged the uncompleted growth of the (0 0 1) plane on ZnO nanosheet surfaces. These results together indicate that the growth on the (0 0 1) plane was suppressed in our system, leading to sheet structures. The ratio between the average length of the parallelogram and the thickness of the nanosheets was determined to be around 100 which is higher than that in other reported ZnO nanodiscs.

The formation of the parallelogram-shaped nanosheets was dependent on several parameters: the reactants, the solvent, the temperature and the stirring. HMT is a good reactant for synthesising metal oxide nanosheets [37,38], and it can also be used to synthesise ZnO nanosheets. However, no water-based methods are reported for synthesising parallelogram-shaped ZnO nanosheets using HMT as one of the reactants. In our experiment, if water was used as the solvent instead of ethanol, ZnO nanowires were formed instead of nanosheets. In addition, the ethanol concentration was crucial: for 99.5% ethanol as a solvent, ZnO polycrystalline clusters were formed (as shown in Supplementary Materials Fig. S2). This means that the solvent content is crucial for the formation of parallelogram-shaped ZnO nanosheets. The temperature parameter controls the dissolving speed of the reactants and the reaction speed [28]. The reactants were not pre-dissolved before mixing; instead, the solid materials were weighed and added into the reaction solvent. The dissolving speed is much slower than in a water solution as observed, leading to a lower reaction speed because the dissolved reactants were less than those in water solution. When the temperature deviated from the ideal 60 °C and was higher (such as 68 °C and 80 °C) or lower (such as 55 °C), more irregular-shaped nanosheets were formed (see images in Supplementary Materials, Figs. S3–S5). If the solution boiled, the final product was ZnO nanoparticles (data not shown) instead of nanosheets. The third parameter, stirring, was also important for the formation of the parallelogram structure. Under the condition of no stirring, a mixture of nanowire, nanosheets and nanorods were found to be the final products (data not shown). One reason for this might be that stirring generates a shear force that breaks ZnO flakes from larger clusters. The angle of the parallelogram-shaped ZnO nanosheets constitutes an interesting phenomenon that needs more research. We suggest that the narrow distribution of the parallelogram angle (97–99°) is due to the different growth rates at different crystal facets.

4. Conclusions

In summary, we reported here on a simple one-step method to synthesise parallelogram-shaped dispersed single-crystalline ZnO nanosheets with an aspect ratio of 1:100, using ethanol as a solvent. The average thickness of the synthesised ZnO nanosheets was 30 nm. The parallelogram angles were found to be narrowly distributed between 97° and 99°. XRD showed a wurtzite structure of ZnO nanosheets. A possible growth mechanism of this parallelogram nanosheets was suggested based on our experimental results. The method here is the first one to report on the synthesis of dispersed parallelogram ZnO nanosheet with sizes up to 150 μm^2. The method here is a simple but efficient way to synthesise regular-shaped ZnO nanosheets, with potential importance for making ZnO nanosheet-based devices.

Acknowledgements

This work was supported by the KKS foundation, the European regional development fund and Länsstyrelsen.

Appendix A. Supplementary data

Supplementary material related to this article can be found, in the online version, at http://dx.doi.org/10.1016/j.mseb.2013.12.009.

References

[1] E.A. Meulenkamp, J. Phys. Chem. B 102 (1998) 5566–5572.
[2] L. Chen, J. Xu, J.D. Holms, M.A. Morris, J. Phys. Chem. C 114 (2010) 2003–2011.
[3] Y.C. Kong, D.P. Yu, B. Zhang, W. Fang, S.Q. Feng, Appl. Phys. Lett. 78 (2001) 407–409.
[4] B.D. Yao, Y.F. Chan, N. Wang, Appl. Phys. Lett. 81 (2002) 757–759.
[5] L. Vayssieres, Adv. Mater. 15 (2003) 464–466.
[6] D.S. Boyle, K. Govender, K. O'Brien, Chem. Commun. 1 (2002) 80–81.
[7] A. Kajbafvala, M.R. Shayegh, M. Mazloumi, S. Zanganeh, A. Lak, M.S. Mohajerani, S.K. Sadrnezhaad, J. Alloys Compd. 469 (2009) 293–297.
[8] A. Kajbafvala, S. Zanganeh, E. Kajbafvala, H.R. Zargar, M.R. Bayati, S.K. Sadrnezhaad, J. Alloys Compd. 497 (2010) 325–329.
[9] J.-H. Park, H.-J. Choi, Y.-J. Choi, S.-H. Sohn, J.-G. Park, J. Mater. Chem. 14 (2004) 35–36.
[10] J. Na, B. Gong, G. Scarel, G.N. Parsons, ACS Nano 3 (2009) 3191–3199.
[11] J.-I. Hong, J. Choi, S.S. Jang, J. Gu, Y. Chang, G. Wortman, R.L. Snyder, Z.L. Wang, Nano Lett. 12 (2012) 576–581.
[12] J.Q. Hu, Y. Bando, J.H. Zhan, Y.B. Li, T. Sekiguchi, Appl. Phys. Lett. 83 (2003) 4414–4416.
[13] C. Kim, Y.-J. Kim, E.-S. Jang, G.-C. Yi, H.H. Kim, Appl. Phys. Lett. 88 (2006) 093104.
[14] Z.-H. Liang, Y.-J. Zhu, G.-F. Cheng, Y.-H. Huang, J. Mater. Sci. 42 (2006) 477–482.
[15] M. Fu, J. Zhou, Q. Xiao, B. Li, R. Zong, W. Chen, J. Zhang, Adv. Mater. 18 (2006) 1001–1004.
[16] F. Xu, M. Dai, Y. Lu, L. Sun, J. Phys. Chem. C 114 (2010) 2776–2782.
[17] E.M.C. Fortunato, P.M.C. Barquinha, A.C.M.B.G. Pimentel, A.M.F. Goncalves, A.J.S. Marques, L.M.N. Pereira, R.F.P. Martins, Adv. Mater. 17 (2005) 590–594.
[18] K. Okazaki, D. Nakamura, M. Higashihata, P. Iyamperumal, T. Okada, Opt. Exp. 19 (2011) 20389–20394.
[19] S. Baruah, J. Dutta, Sci. Technol. Adv. Mater. 10 (2009) 013001.
[20] S.J. Chen, Y.C. Liu, C.L. Shao, R. Mu, Y.M. Lu, J.Y. Zhang, D.Z. Shen, X.W. Fan, Adv. Mater. 17 (2005) 586–590.
[21] J. Guo, J. Zheng, X.Z. Song, K. Sun, Mater. Lett. 97 (2013) 34–36.
[22] T. Taniguchi, K. Yamaguchi, A. Shigeta, Y. Matsuda, S. Hayami, T. Shimizu, T. Matsui, T. Yamazaki, A. Funatstu, Y. Makinose, N. Matsushita, M. Koinuma, Y. Matsumoto, Adv. Funct. Mater. 23 (2013) 3140–3145.
[23] S. Vempati, J. Mitra, P. Dawson, Nanoscale Res. Lett. 7 (2012) 470.
[24] C.X. Xu, X.W. Sun, Z.L. Dong, M.B. Yu, Appl. Phys. Lett. 85 (2004) 3878–3880.
[25] F. Li, Y. Ding, P. Gao, X. Xin, Z.L. Wang, Angew. Chem. Int. Ed. 43 (2004) 5238–5242.
[26] D. Chu, Y. Zeng, D. Jiang, Mater. Res. Bull. 42 (2007) 814–819.
[27] M. Wang, S.H. Hahn, J.S. Kim, J.S. Chung, E.J. Kim, K.-K. Koo, J. Cryst. Growth 310 (2008) 1213–1219.
[28] Z.R. Tian, J.A. Voigt, J. Liu, B. McKenzie, M.J. McDermott, M.A. Rodriguez, H. Konishi, H. Xu, Nat. Mater. 2 (2003) 821–826.

[29] B. Cao, W. Cai, Y. Li, F. Sun, L. Zhang, Nanotechnology 16 (2005) 1734–1738.
[30] Y.G. Sun, J.A. Rogers, Adv. Mater. 19 (2007) 1897–1916.
[31] R.Y. Zhang, H.A. Andersson, M. Andersson, B. Andres, H. Edlund, P. Edström, S. Edvardsson, S. Forsberg, M. Hummelgård, N. Johansson, K. Karlsson, H.-E. Nilsson, M. Norgren, M. Olsen, T. Uesaka, T. Öhlund, H. Olin, Sci. Rep. 3 (2013) 1477.
[32] Y.-I. Jung, B.-Y. Noh, Y.-S. Lee, S.-H. Baek, J.H. Kim, I.-K. Park, Nanoscale Res. Lett. 7 (2012) 43.
[33] V.A. Coleman, C. Jagadish, in: C. Jagadish, S.J. Pearton (Eds.), Zinc Oxide Bulk, Thin Films and Nanostructures: Processing, Properties and Applications, Elsevier, Amsterdam, 2006, pp. 1–20.
[34] S. Zhang, S.-H. Wei, A. Zunger, Phys. Rev. B 63 (2001) 075205.
[35] O.M. Ntwaeaborwa, P.H. Holloway, Nanotechnology 16 (2005) 865–868.
[36] Z.L. Wang, Adv. Mater. 15 (2003) 432–436.
[37] Q.X. Xia, K.S. Hui, K.N. Hui, D.H. Hwang, S.K. Lee, W. Zhou, Y.R. Cho, S.H. Kwon, Q.M. Wang, Y.G. Son, Mater. Lett. 15 (2012) 69–71.
[38] V.K. Ivanov, O.S. Polezhaeva, Russ. J. Inorg. Chem. 54 (2009) 1528–1530.